Value of deterministic day-ahead forecasts of PV generation in PV + Storage operation for the Australian electricity market

Mathieu David, John Boland, Luigi Cirocco, Philippe Lauret, Cyril Voyant

▶ **To cite this version:**

Mathieu David, John Boland, Luigi Cirocco, Philippe Lauret, Cyril Voyant. Value of deterministic day-ahead forecasts of PV generation in PV + Storage operation for the Australian electricity market. Solar Energy, 2021, 224, pp.672-684. 10.1016/j.solener.2021.06.011 . hal-03996042

HAL Id: hal-03996042
https://hal.science/hal-03996042

Submitted on 13 Jun 2023

HAL is a multi-disciplinary open access archive for the deposit and dissemination of scientific research documents, whether they are published or not. The documents may come from teaching and research institutions in France or abroad, or from public or private research centers.

L'archive ouverte pluridisciplinaire **HAL**, est destinée au dépôt et à la diffusion de documents scientifiques de niveau recherche, publiés ou non, émanant des établissements d'enseignement et de recherche français ou étrangers, des laboratoires publics ou privés.

Value of deterministic day-ahead forecasts of PV generation in PV+Storage operation for the Australian electricity market

Mathieu David[a,*], John Boland[b], Luigi Cirocco[b], Philippe Lauret[a], Cyril Voyant[c]

[a] *University of La Réunion - PIMENT laboratory, 15, avenue René Cassin, 97715 Saint-Denis, Reunion*
[b] *Industrial AI, Centre for Industrial and Applied Mathematics, UniSA STEM, University of South Australia, Mawson Lakes Boulevard, Mawson Lakes, SA 5095, Australia*
[c] *Sciences for Environment laboratory, UMR CNRS 6134, University of Corsica Pasquale Paoli, Ajaccio, France*

Abstract

During the last decade, numerous solar forecasting tools have been developed to predict the energy generation of photovoltaic (PV) farms. The quality of solar forecasts is assessed by comparing predictions with measured solar data. However, this methodology does not consider the added value of the forecasts for their applications. As a consequence, what value could be given to the improvement of forecasts considering this evaluation framework?

To answer this question, this work compares the value of different operational solar forecasts for a specific application. The aim is to look for relationships between the economic value and the error metrics defined to evaluate the forecast quality.

A new generation of large-scale PV plants integrates ESS. The aim is to add flexibility to the injection of the production into the grid and thus to maximize the profit by taking advantage of the possibilities offered by the electricity market, such as energy arbitrage. To optimize the operation of these specific ESS, forecasting of the solar production is of paramount importance. The study case considered in this work is a large-scale PV farm of several megawatts associated with Li-ion batteries in the Australian energy market context.

For this specific case study, the results show that the metrics used to evaluate the forecast quality based on the mean absolute error (MAE) have an almost linear relationship with the economic gain brought by applying the forecast. More precisely, an improvement of 1% point in MAE results approximately in an increase of 2% points in economical gain.

Keywords: large-scale PV, energy storage, solar forecasting assessment, operation scheduling, optimization, electricity market, forecast value

*corresponding author

Email addresses: mathieu.david@univ-reunion.fr (Mathieu David), john.boland@unisa.edu.au (John Boland), lui.cirocco@unisa.edu.au (Luigi Cirocco), philippe.lauret@univ-reunion.fr (Philippe Lauret), cyrilvoyant@gmail.com (Cyril Voyant)

1. Introduction

Solar forecasts for horizons ranging from several minutes to several days ahead are available and well documented in the literature. Numerous state of the art studies on the topic have already been published during the past 10 years (Diagne et al., 2013; Antonanzas et al., 2016; Sobri et al., 2018). Currently, the performances of the forecasts are estimated by comparing the forecasts with measurements of solar irradiation or energy production of an associated system (PV, CSP, etc.) (Perez et al., 2013; Blaga et al., 2019; Yang et al., 2020). A common framework based on this testing approach is widely used by the academic community in the realm of solar forecasting. The main error metrics are the Mean Bias Error (MBE), the Root Mean Square Error (RMSE), the Mean Absolute Error (MAE) and the forecast skill based on the RMSE (Coimbra et al., 2013). Solar forecasts are produced to anticipate the future production of solar renewables, to improve grid operation and to decrease the cost of energy production. Indeed, they are important inputs to optimize the scheduling of unit commitments for grid management or to achieve the optimal control of Energy Storage System (ESS) needed to add flexibility to solar renewables. As a consequence, the value of solar forecasts must also be evaluated with reference to their use.

A gap currently exists between the developers of solar forecasts and the community that develops algorithms to integrate them into energy and power management systems (EMS and PMS) such as an optimal controller of ESS. On one hand, solar forecasts are evaluated without considering their added value for the users (Perez et al., 2013; Blaga et al., 2019; Yang et al., 2020). As a consequence, the improvement of solar forecasts are mainly driven by the reduction of the square error between the predictions and the observations. On the other hand, even if several works propose operational solar forecast as input of optimization methods used to manage energy systems (Ramahatana and David, 2019; Faraji et al., 2020; Pousinho et al., 2014; Iliadis, Petros et al., 2019), only few of them consider their added value or assess the gain of an enhancement of the forecasts (Wittmann et al., 2008; Kraas et al., 2011). In the domain of microgrids, where the literature about optimal control of ESS is abundant, real forecasts are even seldom used. Most of the works use historical records as "perfect forecasts" (Riffonneau et al., 2011; Nguyen et al., 2009; Luu et al., 2015; Morais et al., 2010; Wouters et al., 2015) or perturbed measured data (Abdulla et al., 2018; Bridier et al., 2016; Choi and Min, 2018). As a consequence, results are missing an accurate idea of the value of actual solar forecasts.

As mentioned above, forecasts for solar PV farms are typically assessed on the accuracy of the prediction to actual performance, rather than in the effectiveness of the generation system in delivering a desirable financial objective. Currently, the RMSE and the forecast skill also based on the RMSE initially proposed by Coimbra et al. (2013) tend to be the most predominant error metrics used in the academic literature to rank solar deterministic forecasts (Blaga et al., 2019; Yang et al., 2020). The estimation of the market value requires one to model and to simulate the selected application. Such a process is expensive in both time and calculation means. Some propositions exist to assess the economic value of weather forecasts without simulating the system. They are based on the cost caused by an error of forecasts such as the cost-loss function approach proposed by Richardson (2000). For

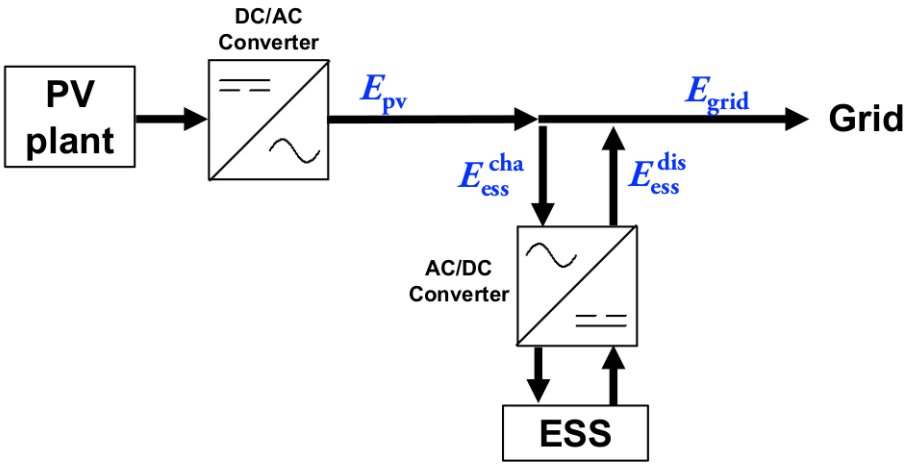

Figure 1: Schematic of the system model. The exchanged energy used to model the balance of the system (see Eq. 1) are given in blue font. The arrows indicate the direction for positive valued energy flows.

instance, this method is relevant to assess the economic performance of renewable production forecasts in the case of energy trading when the cost of an error of forecasts is perfectly known. However, when an ESS is introduced in the system, adding the possibility to shift the energy production, the problem becomes more complex and this simple approach is not suitable.

The aim of the present work is to evaluate the quality and the value of different state of the art solar forecasts. First, the assessment of quality will be done with the framework commonly used by the solar community. Then, we will evaluate the value of the forecasts for a specific application: the day-ahead scheduling of an ESS associated with a large-scale PV plant in the Australian electricity market context. Finally, we will highlight the link between the error metrics commonly used to assess the quality of forecasts and their impact on the economic of the selected application.

The remainder of this article is organized as follows. The next section details the system that is studied and its associated models. Section 3 presents the optimization problem and how the forecasts are implemented. Then Section 4 describes the measured and forecast data used to simulate the case study. Section 5 gives the evaluation framework. And finally, Section 6 presents the results and the associated discussion.

2. System model

The ESS integration selected for this work aims at increasing the revenue of a large-scale PV farm using the bulk energy price arbitrage of the Australian National Electricity Market (NEM). The goal of an energy arbitrage strategy is to benefit from the variations

of the electricity prices, i.e. to buy energy when the price is low and to sell it when it is more profitable. The Hornsdale Power Reserve (HPR), built by Tesla and located at the Hornsdale Wind Farm in Jamestown, South Australia, well illustrates this type of ESS usage. Indeed the main source of revenue of the HPR comes from energy arbitrage. It is also worth noting that non negligible additional revenue of the HPR comes from contingency frequency control ancillary services (FCAS) (Aurecon Group, 2020). An extensive literature focused on the use of storage for energy arbitrage in the context of increasing penetration of intermittent renewable exists. For instance, Zhao et al. (2015) give an overview on the topic but restricted to wind farms and Berrada and Loudiyi (2016) extend the review to take into account the PV plants.

In this work, the storage is added to a PV farm to firm and to shift in time the PV generation in order to benefit from better selling prices. A classical type of PV and storage coupling is assumed. The ESS is connected to the AC bus between the PV farm and the grid connection point (see Fig. 1). With this configuration, the total power of the system is not limited by the maximum power of the inverter of the PV plant. However, to benefit from possible investment tax credit (ITC) (IRENA, 2020), the ESS will charge exclusively with the energy generated by the PV plant. The EMS controls the system and aims at maximizing the revenue provided by the electricity generation. The energy balance of the system is given by the following equation:

$$E_{\text{grid}} = E_{\text{pv}} - E_{\text{ess}}^{\text{cha}} + E_{\text{ess}}^{\text{dis}}, \tag{1}$$

where E_{pv} and E_{grid} are respectively the energy produced by the PV field and the energy supplied to the grid. And $E_{\text{ess}}^{\text{cha}}$ and $E_{\text{ess}}^{\text{dis}}$ correspond to the charge and discharge of the storage system. In the following subsection details are given of the different models used to compute these energies.

2.1. PV system model

Detailed models of PV systems, such as the ones proposed in the pvlib package (Holmgren et al., 2018), could produce very accurate results in comparison with real systems but they also require a detailed description of the system components (i.e. PV modules and inverters). As highlighted by Mayer and Gróf (2021), the choice of the PV system model has a little impact on the accuracy of the whole chain of conversion ranging from the available solar resource to the PV system generation. Furthermore, as the case study is an imaginary case, the PV system model will be used to compute both the real PV production and the forecasted PV production. Thus, we propose here to use simple but efficient models for the PV system as they offer the best trade-off between complexity of implementation of the PV model and accuracy of the results of the study.

The direct current (DC) PV production $E_{\text{pv}}^{\text{DC}}$ is computed with a simple model proposed by Luque and Hegedus (2011). This model takes into account the solar energy received on the tilted plane of the solar modules, so called global tilted irradiation (GTI in Wh/m^2), and the temperature of the modules T_{pv}. Eq. (2) and (3) give the computation details. The temperature of the modules (Eq. (2)) depends on the ambient temperature T_{air}, the

Parameter	Value
Area (A)	1.64 m^2
Efficiency at STC (η_{pv}^{STC})	0.195
Temperature coefficient (TC_{pv}^{STC})	-0.0038 $°C^{-1}$
Temperature NOCT (T_{pv}^{NOCT})	46 °C
Total installed costs (C_{pv})	2175 AUD/kW

Table 1: Characteristics of the modules LG NEON2 320 Wp and utility-scale PV costs in Australia (IRENA, 2019)

temperature of the module observed under the nominal operating cell temperature T_{pv}^{NOCT} and the received irradiance GTI. Then Eq. (3) computes the PV production, with A the area of the PV plant, η_{pv}^{STC} the efficiency and TC_{pv}^{STC} the temperature coefficient of the selected modules under the standard test conditions (STC). For our case study, we chose modules LG NEON2 with a peak power of 320 W because this model is currently very popular in Australia. Table 1 presents the main characteristics of this module, which are used in Eqs. (2) and (3):

$$T_{pv} = T_{air} + (T_{pv}^{NOCT} - 20) \times GTI/800, \tag{2}$$

$$E_{pv}^{DC} = GTI \times A \times \eta_{pv}^{STC} \times (1 - TC_{pv}^{STC} \times (T_{pv} - 25)). \tag{3}$$

Even if we assume a large-scale PV plant with a peak power of at least several megawatts, the production will be derived from a PV system of 1 MWp, i.e. 3125 modules for a total area of approximately 5000 m^2. This specific installed power will allow normalizing all the results.

To compute the AC output of the PV plant ($E_{pv} = \eta_{inv} E_{pv}^{DC}$), the simple inverter model proposed by Riffonneau et al. (2011) has been used. A second order polynomial of the DC power ratio r estimates the global efficiency of the inverter η_{inv} as follow:

$$\eta_{inv} = 1 - (0.0094 + 0.043r + 0.04r^2)/r, \tag{4}$$

$$r = \frac{E_{pv}^{DC}}{\Delta t P_{inv}}. \tag{5}$$

In Riffonneau et al. (2011), the DC power ratio of the inverter r is the ratio between the DC PV power and the nominal power of the inverter P_{inv}. Here, we assume that the DC output power of the PV farm is constant during a time step Δt and can be easily derived from the produced DC energy as indicated in Eq. (5). To take into account the working limits of the inverter, we also set its start-up at 10% and its clipping at 110% of the nominal power P_{inv} as observed by King et al. (2007). Hence, when the ratio r is below 0.1 the inverter does not work and when r is above 1.1 the inverter caps the production. Finally, we define a rated power of the inverter equal to the installed capacity of PV (i.e. an inverter of 1 MW for 1 MWp of PV). For grid connected systems, it is common to have the inverter rating match or be slightly smaller than the peak installed PV capacity (Luque and Hegedus, 2011).

2.2. ESS model

Numerous technologies of ESS are currently available. They are commonly classified regarding their capacity, power and response time. With few hours of production per day and fast variations of their output, PV systems require ESS with very short response time and with a power in the same order of magnitude of the installed power. Electrochemical batteries and more specifically Li-ion ones are currently the most affordable ESS that possess these properties. Thus, as many PV operators, we naturally choose to use Li-ion batteries. The power units associated to the batteries are AC/DC converters. In this work, we assume a constant efficiency for these converters. The current and expected future characteristics of the selected ESS model were derived from a recent report published by the International Renewable Energy Agency (IRENA, 2017) and they are given in Table 2[1]. The self-discharge of the Li-ion batteries, around 0.1% per day, is neglected because we assume that the ESS will realize almost a full-cycle every day.

To compute the energy transfers corresponding to a variation of the state of charge ΔSOC of the ESS, we applied the round trip efficiency to the charging phase while the discharge is only subject to the efficiency of the AC/DC converter. Eqs. (6) and (7) below detail how the charging and discharging energies are obtained:

$$E_{\text{ess}}^{\text{cha}} = \frac{\Delta SOC_{\{\Delta SOC>0\}}}{\eta_{\text{ess}}^{\text{cha}} \times \eta_{\text{ess}}} \times ESS_{\text{capa}}, \tag{6}$$

$$E_{\text{ess}}^{\text{dis}} = -\Delta SOC_{\{\Delta SOC<0\}} \times \eta_{\text{ess}}^{\text{dis}} \times ESS_{\text{capa}}, \tag{7}$$

where ESS_{capa} is the rated capacity of the ESS and $\eta_{\text{ess}}^{\text{cha}}$, $\eta_{\text{ess}}^{\text{dis}}$ and η_{ess} are respectively the charging, discharging and round-trip efficiency of the ESS. Their values are given in Table 2. As a discharge corresponds to a negative variation of the SOC (i.e. $\Delta SOC < 0$), one can notice that a minus is added to Eq. (7) to obtain a positive energy of discharge $E_{\text{ess}}^{\text{dis}}$ and thus to be coherent with the Eq. (1) about the energy balance of the overall system.

The ageing model proposed by Riffonneau et al. (2011) is used to evaluate the level of degradation of the batteries. This model is simple and appealing. Indeed, it assumes a linear degradation of the capacity of the batteries that can be applied to a large number of technologies. Let's consider a discharge of the ESS corresponding to the decrease of the state of charge $\Delta SOC_{\{\Delta SOC<0\}}$. The associated reduction of the state of health ΔSOH is

$$\Delta SOH = z \times \Delta SOC_{\{\Delta SOC<0\}}. \tag{8}$$

In the Eq. (8) above z is the ageing coefficient that can be derived from the ESS life time CLF expressed in number of full cycles and from the corresponding reduction of the state of health of the ESS as follows

$$z = \frac{SOH_0 - SOH_{\min}}{CLF \times ESS_{\text{capa}}}, \tag{9}$$

[1] An exchange rate of 1.4 USD/AUD has been used to convert the capital expenditures (CAPEX) and operating expenses (OPEX) proposed in (IRENA, 2017).

Parameter	Value		
	2020	**2025**	**2030**
Round trip efficiency (η_{ess})	0.955	0.961	0.968
State of charge ($SOC_{\max}$ and $SOC_{\min}$)	1 - 0.1	1 - 0.1	1 - 0.1
Charging ($\eta_{\text{ess}}^{\text{cha}}$) / Discharging efficiency ($\eta_{\text{ess}}^{\text{dis}}$)	0.98	0.98	0.98
Power unit limit ($P_{\max}^{\text{cha}}$ / $P_{\max}^{\text{dis}}$)	3.5 W/Wh	3.5 W/Wh	4 W/Wh
Life time in equivalent full-cycles (CLF)	2406	3032	3820
State of health (SOH_0 and $SOH_{\min}$)	1 - 0.8	1 - 0.8	1 - 0.8
ESS cost ($C_{\text{ess}}^{\text{capa}}$)	452 AUD/kWh	325 AUD/kWh	234 AUD/kWh
Conversion units cost ($C_{\text{ess}}^{\text{power}}$)	119 AUD/kW	92 AUD/kW	70 AUD/kW
Annual O&M costs ($C_{\text{ess}}^{\text{om}}$)			1.5% of investment cost

Table 2: Current and future characteristics of Li-ion NMC (cathode combination Nickel-Manganese-Cobalt) batteries and of the associated AC/DC power units (IRENA, 2017).

where SOH_0 and $SOH_{\min}$ are respectively the initial and critical state of health of the ESS. Their values are given in Table 2. This model will be used during the simulations to decrease the actual ESS capacity after every discharge. Furthermore, the ESS should be changed when the SOH reaches $SOH_{\min}$ and the corresponding cost should be added to the operation costs. But, in our study case we will consider a 10 years period for the economical analysis (see Subsection 5.2) and $SOH_{\min}$ will not be reached.

2.3. Grid model

The electricity produced by the production system is sold to the grid at the spot price (C_{grid}). We assume that the grid operator will buy the whole supplied energy. Furthermore, the size of the considered power plant is not significant enough to influence the spot prices of the electricity market. The Australian Energy Market Operator (AEMO) defines the spot price as the selling price of electricity for the energy producers. It corresponds to an average price computed every half-hour. The details of the computation of the spot price are given in AEMO Markets (2018).

3. Data

3.1. Ground measurements

The ground measurements correspond to two consecutive years (2016 and 2017) of air temperature (T_{air}), Global Horizontal Irradiation (GHI), Beam Normal Irradiation (BNI) and Diffuse Horizontal Irradiation (DHI) measured at Adelaide Airport (34.95° N, 138.51° S). The site experiences a Mediterranean climate with a significant annual GHI of approximately 1760 kWh/m^2/year. The initial sample rate of the records is 1 minute and an averaging was applied to the data to obtain 30 minute means. Considering only the daylight hours, the raw measurements present less than 1% of missing data. The shorter gaps, corresponding to a maximum of 30 minutes, were filled by linear interpolation. The longer gaps, (e.g. there is a gap of 3 consecutive days between January and February 2017) were filled with GHI estimations corresponding to the same period from the MERRA-2 reanalysis available for

free via the SoDa portal (MINES ParisTech, 2020). The comparison between the MERRA-2 estimations and the 2 years of data used in this work gives a mean bias error (see Eq. 18) of +7%. This result is consistent with assessments done for other regions (Zhang et al., 2020). Considering the very small rate of missing data and this slight overestimation of the MERRA-2 data, we assume that the gap filling will not affect the overall results of the study.

No PV generation was recorded on-site as the study case is an imaginary power plant of 1MWp with storage. We assume PV panels facing North and and inclined at 35°, which is the tilt that maximizes the annual solar energy received on the plane of the PV modules. The solar energy received on the PV modules (GTI), is derived from the measured GHI, DHI and BNI by using a transposition model. Here we use the anisotropic transposition model proposed by Hay and Davies (1980) with an albedo of 0.2. Then, from the GTI and the measured air temperature (T_{air}), the PV output is computed with the PV model depicted in Section 2.1. According to Hofmann and Seckmeyer (2017), the estimation of the PV production by the combination of selected models results in a very low mean error (less than 2% in average).

3.2. Forecasts

The goal of this work is to analyse the effect of the error of solar forecasts on the revenues of the selected system. The scheduling optimization studied here requires day-ahead forecasts of the PV generation profile with a 30-min time step. Regarding this horizon of forecast, Numerical Weather Predictions (NWPs) are the most suitable (Diagne et al., 2013; Antonanzas et al., 2016). Indeed, they commonly exhibit the best accuracy for forecast horizons ranging from 6 hours to several days ahead. NWPs are commonly associated with post-processing methods that permit decreasing their error when compared with GHI ground measurements. To generate the PV production forecasts from the GHI ones, the following combination of models is required:

1. A decomposition model that divides the GHI in the beam (BNI) and diffuse (DHI) components of the solar irradiance;
2. A transposition model that computes the solar energy received on the plane of the PV modules (GTI) from the GHI, BNI and DHI;
3. And a PV production model that converts the received solar energy in electricity generation.

3.2.1. GHI Forecasts

The short-term NWPs of the GHI used in this work are provided by the European Centre of Medium-range Weather Forecasts (ECMWF) (Leutbecher and Palmer, 2008) and National Centers for Environmental Prediction (NCEP) (NCEP, 2015). The ECMWF maintains and runs the Integrated Forecast System (IFS). IFS is a global high resolution NWP model that generates weather forecasts for the entire earth with a spatial resolution of 0.125° in both latitude and longitude and temporal resolution of 1 hour for the 4 first days of forecast. The NCEP also runs a global NWP model called GFS (Global Forecast System). However,

GFS exhibits a coarser resolution than the IFS model with a spatial resolution of 0.250° and temporal resolution of 3 hours for the 4 first days of forecasts. The GHI forecasts with a lead-time of up to 4 days were retrieved from the nearest pixel to the Adelaide airport. To be consistent with the Australian market rules, i.e. a 30-min time granularity (see Section 2.3), the raw forecasts need to be downscaled. For instance, the forecasts of the NCEP, which have a time step of 3 hours, must be converted into a 30-min time series. Several methods of oversampling exist such as the linear, cubic or spline interpolations or the nearest neighbors approach proposed by Mueen et al. (2017) and used by Yang et al. (2019a) to downscale NWPs. If these techniques are suitable to downscale most of the meteorological parameters, they are not appropriate to solar irradiation time series as mentioned by Blanc and Wald (2010). Indeed, the energy of the oversampled time series is not equal to the original time series. In this work, we used the method proposed by the ENDORSE project (Espinar et al., 2011). Based on iterative linear interpolations, this method has been designed specifically to downscale time series of solar data. The method respects an energy consistency property and therefore, in terms of energy, the oversampled time series is equal to the original time series. Thus, the downscaling does not add additional bias to the new time series.

As proposed by the literature about solar forecast evaluation, a reference model, the persistence, is also used (Sengupta et al., 2017). Several versions of the persistence are available (Yang, 2019). In this work, we use the day ahead persistence of the clear sky index ($kt^*Persistence$): the daily profile of the clear sky index of the current day is repeated for the next days. Compared to the GHI persistence, the $kt^*Persistence$ takes into account the seasonal evolution of the solar path and it provides slightly better results. The clear sky irradiances needed to compute the clear sky index were provided by the McClear model (Lefèvre et al., 2013) available for free on the SoDa website (Atmosphere Monitoring Service, 2020). This model uses the Aerosol Optical Depth (AOD), water vapor and ozone data from the MACC project.

3.2.2. PV Forecasts

The forecasts of the direct current PV generation are derived from the GHI forecasts via the combination of a decomposition model, a transposition model and a PV model. We explained previously that the PV production of reference was computed using the transposition model proposed by Hay and Davies (1980) and the PV model developed by Luque and Hegedus (2011). The same models will be used to obtain the PV forecasts. Regarding the decomposition of the GHI, we propose to test two state-of-the-art models. Indeed, the decomposition of the GHI is one of the main source of error to derive the GTI and as consequence to compute the PV generation (Gueymard, 2009; Hofmann and Seckmeyer, 2017; Mayer and Gróf, 2021). The first model is the well-known Erbs model (Erbs et al., 1982). This model, developed forty years ago and based only on the clearness index, combines simplicity and accuracy. Furthermore, it is widely used by the community and thus appears to be a very good competitor for comparison studies, (Hofmann and Seckmeyer, 2017; Mayer and Gróf, 2021). Second, we used the decomposition model developed by Boland, Ridley and Lauret, so called BRL, initially developed in Adelaide (Ridley et al., 2010). This more recent and more complex model considers multiple predictors as inputs. It is also widely

Raw NWPs	Post-processed NWPs			
ECMWF	before PV conversion	ECMWF-WBb	ECMWF-NNb	ECMWF-PARb
	after PV conversion	ECMWF-WBa	ECMWF-NNa	ECMWF-PARa
NCEP	before PV conversion	NCEP-WBb	NCEP-NNb	NCEP-PARb
	after PV conversion	NCEP-WBa	NCEP-NNa	NCEP-PARa

Table 3: List of the forecasts derived from the two NWP models considered in this work.

used because it is one of the best models in terms of accuracy (Hofmann and Seckmeyer, 2017; Bertrand et al., 2015) and it is suitable to generate reliable solar forecasts (Mayer and Gróf, 2021).

Using the combination of models described in the previous paragraph, we derived PV predictions from the GHI forecasts of the two considered NWPs (i.e. NCEP and ECMWF) and also from the clear sky index persistence (i.e. $kt^*Persistence$). In addition, we also propose to use the simple day-ahead persistence of the PV output.

3.2.3. Post-processing

Raw NWPs are commonly post-processed to reduce their error. It is worth noting that the aim of the post-treatment is to increase the agreement between the forecasts and the measurements. This does not mean that the post-processed NWPs should produce better PV forecasts for different indicators at the same time (e.g. quality and value). To evaluate this assumption, we propose to test three different post-processing methods. The first technique produces a forecast without bias (noted WB) by simply subtracting the mean bias error (see Eq. 18) from the raw NWPs. Second, the bias correction is done by an Artificial Neural Network (noted NN) as proposed by Lauret et al. (2014, 2016). The third method uses a rolling horizon approach based on a periodic autoregressive stochastic process (noted PAR) (Franses and Paap, 1994; Voyant et al., 2018). A systematic description of the NN and PAR methods is given in the appendix. The post-processing techniques presented above will be applied to the NWPs of the GHI but also to the PV forecast derived from the raw NWPs. Indeed, even if the literature in the domain provides mainly results concerning post-processing of the GHI, the energy operators likely prefer to post-process the PV forecasts.

3.2.4. Overview of the forecasts used

We evaluate 31 different forecast models in this work. For reference three persistence models are used: the day-ahead persistence of the PV output (Persistence) and two day-ahead clear-sky persistence (kt^* Persistence) models, one associated the Erbs decomposition and the other with the BRL decomposition. The remaining 28 models are based on 7 forecasts for the PV output, formed from a combination of each of the two NWP models, ECMWF and NCEP, three post processing methods and each of the two decomposition methods, Erbs and BRL. Table 3 presents the 14 combinations of NWP and post-processing options before and after converting to PV output; note that evaluating the raw NWP models "before PV conversion" are not the subject of this work.

4. Formulation of the optimization problem using Linear Programming (LP)

The LP formulation of the optimization problem only requires consideration of linear relationships for the cost function and the constraints. As we assume a constant efficiency of the converter associated to the ESS and also a linear behavior of the batteries, the proposed optimization problem is linear. Five decision variables are considered: the charge ($E_{\text{ess}}^{\text{cha}}$) and discharge ($E_{\text{ess}}^{\text{dis}}$) energy of the batteries, the energy purchased or injected to the grid (E_{grid}), the energy generated by the PV plant (E_{pv}) and the state of charge of the ESS (SOC). The objective to maximize is the revenue generated by the energy supplied to the grid and it is stated as

$$R(E_{\text{pv}}, E_{\text{ess}}^{\text{dis}}, E_{\text{ess}}^{\text{cha}}, E_{\text{grid}}, SOC) = \sum_{t=1}^{T} C_{\text{grid}}(t) E_{\text{grid}}(t), \tag{10}$$

where C_{grid} is the spot price of electricity and T is the number of considered time steps. In our case study, we run the optimization for the next three days with a time granularity (Δt) of 30 minutes. So we have $T = 144$ time steps. The objective is subject to the following constraints:

- The boundaries of the decision variables, which are given by the technical specifications of the different component of the system (see Section 2 and Table 2):

$$0 \leq E_{\text{pv}} \leq E_{\text{pv}}^{\max}, \tag{11}$$

$$0 \leq E_{\text{ess}}^{\text{dis}} \leq P_{\max}^{\text{dis}} \times \Delta t, \tag{12}$$

$$0 \leq E_{\text{ess}}^{\text{cha}} \leq P_{\max}^{\text{cha}} \times \Delta t, \tag{13}$$

$$-\infty \leq E_{\text{grid}} \leq +\infty, \tag{14}$$

$$SOC_{\min} \leq SOC \leq SOC_{\max}. \tag{15}$$

  It is worth noting that the energy generated by the PV plant is here considered as a decision variable. Indeed, the operator could choose to curtail the PV production if this action avoids additional cost, for instance when the spot price is negative. Thereby, the energy generated by the PV plant is bounded by the maximum available production (Eq. (11)).

- The energy balance of the system derived from Eq. (1):

$$E_{\text{pv}} + E_{\text{ess}}^{\text{dis}} - E_{\text{ess}}^{\text{cha}} + E_{\text{grid}} = 0. \tag{16}$$

- And the variation of state of charge between two time steps corresponding to the energy that flows in and out of the ESS:

$$(SOC(t) - SOC(t-1)) \times ESS_{\text{capa}} = \eta_{\text{ess}} \eta_{\text{ess}}^{\text{cha}} E_{\text{ess}}^{\text{cha}} - \frac{E_{\text{ess}}^{\text{dis}}}{\eta_{\text{ess}}^{\text{dis}}}, \tag{17}$$

  with $SOC(0)$ the initial state of charge.

4.1. Implementation of the forecasts

Considering the current Australian regulation, large-scale PV plants with storage of a power of 5 MW or more correspond to scheduled generators which sell their electricity through the spot market (AEMO Markets, 2018). As a consequence, the managers of large-scale PV farms integrated with an energy storage must schedule the output profile of their systems and bid for their prices. Two delivery times are in use. The pre-dispatch, which can be seen as a day-ahead market, requires the submission of the initial production schedule and price bands at 12:30pm of the current day until 12:30pm of the next day with a half-hourly time step corresponding to the period used to compute the settlement price, also called spot price (AEMO System Capability, 2016). As the interval used for the real time dispatch is 5 minutes, generators may submit rebids of their production and prices 5 minutes before the start of the next five-minute dispatch interval (AEMC, 2015). Only the 5 minute rebids are mandatory. The day ahead submission of the production profile is optional but highly recommended for the main energy suppliers. This work focuses on day-ahead forecasts. So, only the pre-dispatch stage will be considered. Furthermore, this study is in agreement with the recent recommendation of the Australian Department of the Environment and Energy to assess the suitability of a day-ahead market (Finkel et al., 2017).

The day-ahead PV production forecasts are implemented in the optimization with a receding horizon approach. Three days of forecasts are used to optimize the schedule of the ESS operation but only the first day of the resulting optimal schedule is used to run the system. Receding horizon is a widely used approach in energy planning (Yang et al., 2019b). Indeed, it permits updating efficiently the operation schedule of the production units when a new forecast is available.

As the forecast is inherently uncertain, the execution of schedule generated by the optimization will obviously generate deviations with the expected energy balance. During the running of the system, these deviations will be compensated by the storage and by curtailing the PV production. In case the storage is empty and the system is not able to ensure the production plan, we assume that the operator will submit a rebid of their production on the 5 minutes market. So, we will not consider penalties in this work.

5. Evaluation framework

Two attributes of the forecasts will be tested in this work. Firstly, we evaluate the agreement between forecasts and observations. Secondly, we establish the value of the forecasts in giving a benefit for the user. Additionally in this section, we will investigate hybrid metrics that straddle the space between quality and value.

5.1. Forecast quality

A framework dedicated to the evaluation of the quality of solar deterministic forecasts is now widely used by the academic community and also by forecast providers. This framework is detailed in numerous works (Perez et al., 2013; Coimbra et al., 2013; Sengupta et al., 2017; Blaga et al., 2019). All the metrics defined in this framework are directly derived from the difference between observations X_{obs} and forecasts $\widehat{X}_{\text{fcst}}$ (Eq. (21)). In this work

we will assess the quality through the Mean Bias Error (MBE, Eq. (18)), the Root Mean Square Error (RMSE, Eq. (19)), the Mean Absolute Error (MAE, Eq. (20)) for a set of N observation/forecast pairs. These metrics are given as:

$$\mathrm{MBE} = \frac{1}{N}\sum_{i=1}^{N} err(i), \tag{18}$$

$$\mathrm{RMSE} = \sqrt{\frac{1}{N}\sum_{i=1}^{N} err(i)^2}, \tag{19}$$

$$\mathrm{MAE} = \frac{1}{N}\sum_{i=1}^{N} \mid err(i) \mid , \tag{20}$$

where

$$err(i) = \widehat{X}_{\mathrm{fcst}}(i) - X_{\mathrm{obs}}(i) \text{ for } i = 1, 2, ..., N. \tag{21}$$

In order to get intelligible results expressed as percentages, these three metrics will be normalized by the mean of observed irradiation and by the installed PV power when they correspond respectively to irradiation forecasts and PV generation forecasts.

The Forecasting Skill (FS) will be also provided in this work. The FS refers to the relative RMSE improvement of a specific method compared to a benchmark forecast (Eq. (22)). The day-ahead persistence of the clear sky index (see Section 3) will be the reference forecast in this work. Even if the FS will give exactly the same information as the RMSE for our case study. The FS, given by

$$\mathrm{FS} = 1 - \frac{\mathrm{RMSE}(method)}{\mathrm{RMSE}(kt^{*}Persistence)}, \tag{22}$$

could be used in comparison studies. Fig. 2 to 4 give a graphical overview of the MBE, RMSE and MAE for the 31 considered PV forecasts. Table 4, which gives the error metrics that quantify the forecast quality, is given at the end of the paper. One can see that the persistence based forecasts experience the worst RMSE and MAE. Most of the forecasts based on the ECMWF model outperform the ones derived from the NCEP model. It is also worth noting that the PAR and NN post-processing methods, which set up a minimization of the square error between observations and forecasts, decrease the RMSE of the raw NWPs. However, they also tend to increase the MAE. As a consequence, a ranking based on the MAE will result in a totally different classification than a ranking based on the RMSE as is commonly done with the FS.

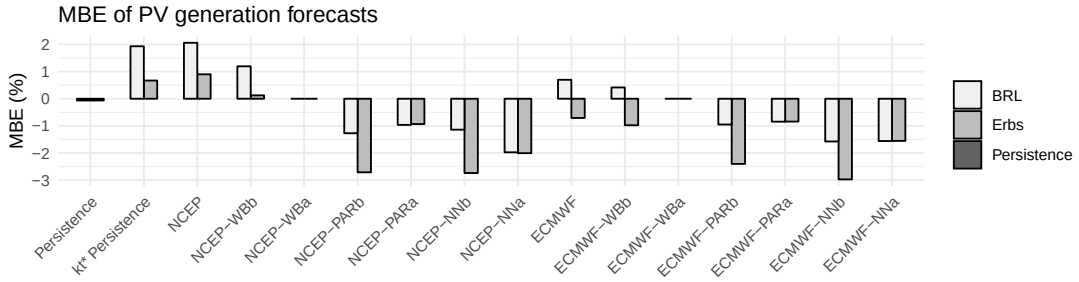

Figure 2: Mean Bias Error (MBE) of the PV production forecasts.

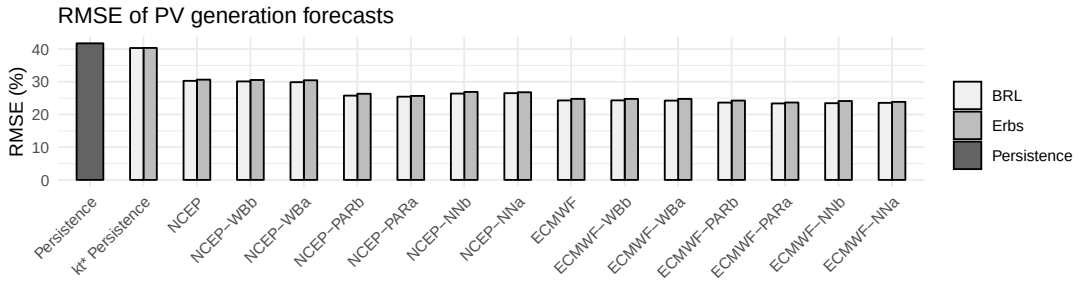

Figure 3: Root Mean Square Error (RMSE) of the PV production forecasts.

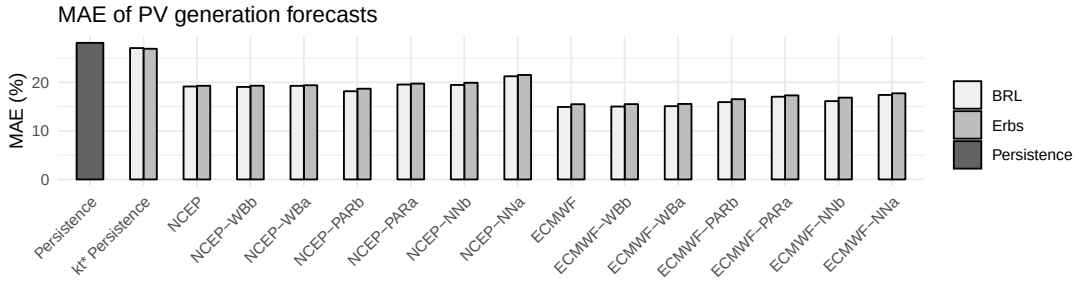

Figure 4: Mean Absolute Error (MAE) of the PV production forecasts.

5.2. Forecast Value

The IRENA recently released a report that defines an Electricity Storage Valuation Framework (ESVF) (IRENA, 2020). This global approach is designed for a large set of end-users such as policy makers, project developers, energy operators, etc. Indeed, both monetisable and non-monetisable benefits are included in the ESVF. This work will only focus on the fourth step of the ESVF dedicated to the simulation of storage operation and to the evaluation of the revenues (i.e. monetisable benefits).

The objective here is to determine the benefits on revenues of the addition to the PV plant of an ESS operated with improved forecasts. Several approaches are proposed in the literature. For instance, the Levelized Cost of Storage (LCOS) evaluates the cost of the energy supply by an ESS to a grid (Pawel, 2014). However, the LCOS does not give a direct quantification of the economic gain provided by the forecast to the owner. In this work, the added value will rely on the difference of revenues of the system with and without ESS as proposed by Fathima and Palanisamy (2015) or Bridier et al. (2016). For our case study, the revenue of reference R_0, is the cash flow generated by the PV farm without storage and consequently without need of forecast. In the Australian context, such a PV farm is a semi-scheduled plant that sells its production at the spot price. We will assume a very optimistic revenue of reference R_0 considering that the whole energy produced by the PV plant will be sold. Considering a simulation of the PV farm without storage using the solar irradiation measurements and the spot prices of 2017, R_0 is 201,629 AUD/year for an installed power of 1 MW. As the scale of the revenue is difficult to interpret, we propose to assess the value of the forecasts with the economic gain. This rate, expressed in percent (Eq. 23) is the relative difference between the revenue of reference R_0 and the revenue of the system with the ESS R, which is the objective function of the optimization problem detailed in Eq. 10 (see Section 4). The economic gain is proportional to the revenue and has the advantage to be easier to interpret and reads as

$$gain = \frac{R - R_0}{R_0} \times 100. \tag{23}$$

In addition to the economic gain, we will compute the Net Present Value (NPV) of the ESS. The NPV is a useful figure to decide whether or not it is of value to invest in the ESS. A negative NPV highlights a bad investment. Whereas, a high value for the NPV is indicative of an important pay back on investment. The NPV computation is based on the methodology defined in the famous report initially published by the NREL in 1995 and released as a book ten years after (Short et al., 2005). Similar to the economic gain, the NPV considered in this work relies only on the additional cash flow generated by the ESS (i.e. $R - R_0$). Fig. 5 shows the evolution of the NPV for an ESS capacity ranging from 0 MWh/MWpv to 3 MWh/MWpv and considering the year of investment in the storage. Perfect forecasts have been used to schedule the ESS operations and to obtain these results. Considering the IRENA prices for the ESS (see Table 2) and the current financial situation (Grant Thornton and Clean Energy Pipeline, 2019), the investment in the ESS should be suitable from 2025. These results must be handled with care because we consider the energy arbitrage as the only source of revenue and the spot price of 2017. However, this point is not the aim of this work and here the NPV will be used to evaluate the optimal size of the ESS, which is around 1.8 MWh/MWpv.

5.3. Intermediate metrics

We can define the intermediate metrics used in this work as a combination of quality and value without the need of simulating the studied energy system. Thus, they could be

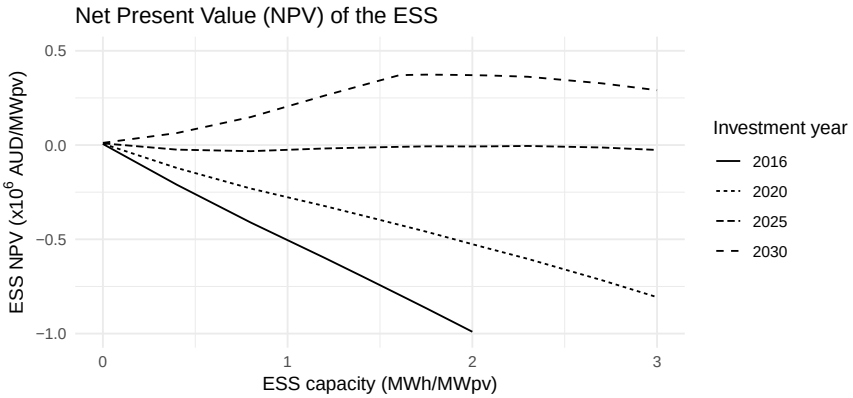

Figure 5: Net Present Value (NPV) of the ESS considering the size of the storage, the year of investment and the current financial situations (5.75% discount rate, inflation rate 2%, 10 years analysis period (Grant Thornton and Clean Energy Pipeline, 2019)).

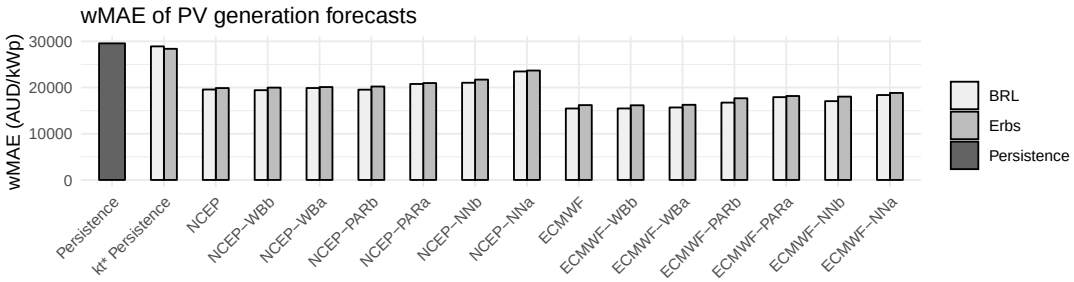

Figure 6: Weighted Mean Aboslute Error (wMAE) of the PV production forecasts.

considered as hybrid indices able to link the quality of the forecast with the added value for the user through a simple approach.

The first intermediate metric proposed in this work is derived from the weighted mean absolute error (wMAE) defined by Antonanzas et al. (2020), which was designed to choose the best solar forecast for market operators. They proposed to weight the absolute error observed at each time step with the downward and upward prices corresponding to the prices at which the system respectively buys and sells electricity to compensate the deviations from the production schedule. In our case, these prices correspond to the spot price (C_{grid}), which fluctuates at each time step and the wMAE is defined in Eq. 24. Errors of forecast weigh heavier when the electricity price is high. Fig. 6 provides an overview of wMAE of the considered PV forecasts. Even if slight differences appear, the wMAE tends to behave like the MAE for our case study. The wMAE is defined by

$$\text{wMAE} = \frac{1}{N} \sum_{i=1}^{N} \mid [\widehat{X}_{\text{fcst}}(i) - X_{\text{obs}}(i)] \times C_{\text{grid}}(i) \mid . \tag{24}$$

Another metric based on the recent work of Perez et al. (2019) will also be studied in this

work. This metric is derived from the concept of "Firm kWh premium" that refers to the Levelized Cost of Energy (LCOE) required to firm the power forecasts through storage and overbuilding of the PV generation capacity. The lower the LCOE, the better the quality of the forecasts. This new metric differs considerably from the previous ones because it does not only consider the instantaneous difference between forecasts and observations. Indeed, the storage size required to firm the PV generation and consequently the capital expense (CAPEX) are highly affected by a succession of large positive or negative errors. Furthermore, assumptions on PV costs, storage costs, maintenance and life time have to be made. For this work, the case study has already fixed most of these parameters (see Tables 2 and 1). In our opinion, a metric based on this approach is worthy of investigation because it straddles the space between quality and value of the forecasts. We propose here a simplified version the "Firm KWh premium" that only takes into account the CAPEX required to firm the forecasts and no loss of energy through the ESS. Indeed, the LCOE is highly dependent on the CAPEX and we want to propose a metric easy to compute that requires a few assumptions. The formulation of the proposed Firm Power Forecasts (FPF) metric, expressed in dollars per installed kilowatts of PV (PV_{power}), is given by the following equation:

$$\text{FPF} = min_{\{osf\}} \left[\frac{(ESS_{\text{capa}} \times C_{\text{ess}}^{\text{capa}} + ESS_{\text{power}} \times C_{\text{ess}}^{\text{power}} + (osf - 1) \times PV_{\text{power}} \times C_{\text{pv}})}{PV_{\text{power}}} \right], \tag{25}$$

where osf is the oversizing factor applied to the actual installed PV power. It is important to note that in this work, the oversizing factor is not applied to a PV capacity required to produce the yearly energy of the forecasts, like in (Perez et al., 2019), but directly to the actual installed PV power. The FPF value results from an easy to solve one-dimensional optimization because the objective function is convex and osf is the unique decision parameter (i.e. the unique parameter to vary). For our case study, the optimal value of osf ranges from 1.1 to 2.2. These two values correspond respectively to the models $kt^*Persistence$ and ECMWF-WBa. For a fixed osf there is a single value of the ESS capacity and power that minimizes the FPF. The following equations give a simple way to compute them:

$$ESS_{capa} = max(pcse(1), ..., pcse(N)), \tag{26}$$

$$pcse(i) = \begin{cases} \sum_{k=1}^{i} pcse(k-1) + err(k) \text{ if } \sum_{k=1}^{i} pcse(k-1) + err(k) > 0 \\ 0 \text{ otherwise,} \end{cases} \tag{27}$$

$$ESS_{\text{power}} = max(\mid pcse(2) - pcse(1) \mid, ..., \mid pcse(N) - pcse(N-1) \mid), \tag{28}$$

$$err(i) = \widehat{X}_{\text{fcst}}(i) - osf \times X_{\text{obs}}(i) \text{ for } i = 1, 2, ..., N. \tag{29}$$

$pcse$ can be interpreted as the positive values of the cumulative sum of the forecasting errors and, in a sense, it refers to the accumulated energy in the ESS. A negative value of

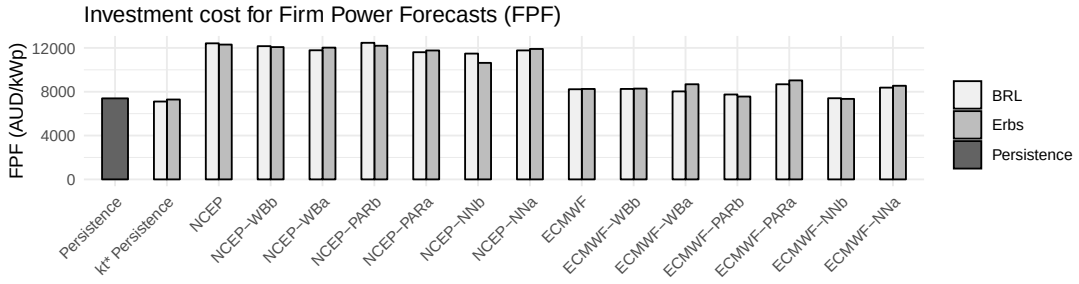

Figure 7: Firm Power Forecast (FPF) of the PV production forecasts.

pcse indicates that we can curtail the production. The error of forecast *err* is exactly the same as in Eq. 21, but in the case of the FPF computation the observed amount of energy is multiplied by the oversizing factor osf.

Fig. 7 gives the FPF for the considered PV forecasts. As it is highly sensitive to successions of positive or negative errors, this intermediate metrics gives a totally different ranking than the other metrics used in this work. Indeed, the persistence based forecasts experience the lowest FPF.

6. Results

First of all, it is important to reiterate that the aim of this work is not to rank the forecasts between them. Such a goal requires consideration of numerous sites and maybe a large variety of applications. The objective here is to show that correlations could exist between metrics defined to assess the quality of point forecasts and the added value brought by an ESS managed with improved forecasts. This is why we generated many different PV forecasts in order to support our results with a significant number of metric/value pairs. In this section are presented graphical views of the results (i.e. scatter plots). Interested readers can refer to Table 4 in the appendix to get the all the corresponding numerical results.

Fig. 8 plots the gain as a function of the MBE (a), the MAE (b) and the RMSE (c), which are currently the three main metrics used to assess the quality of a solar forecast. First, compared to the PV farm alone, the gain provided by the storage managed with day-ahead forecasts ranges from around 25% to more than 55% for the perfect forecast. Thus, an improvement of the forecast can significantly improve the revenue of such a system. Second, we arbitrarily grouped the forecasts by family (i.e. same color and shape for persistence, ECMWF and NCEP based forecasts). Thus, one can easily observe that the relationships between the selected metrics and the economical gain strongly depend on the type of model used to derive the solar forecasts. Finally, the persistence based forecasts, commonly used as a benchmark, give an identical and even slightly better gain than the worst forecasts derived from the NCEP model. However, the forecast skill based on the RMSE (see Table 4) shows a clear improvement of the quality of these forecasts when compared to the persistence.

If we focus on Fig. 8(a), we can observe that a positive bias leads globally to a better revenue in the same family of forecasts. If we look in detail at the rules of the optimization and at the structure of the costs associated to an error of forecast, this result is obvious. Indeed, if an outcome higher than the forecast occurs when the storage is full, the algorithm curtails the PV production. On the contrary, when the ESS is empty, an outcome lower than the forecast is balanced by a purchase from the grid without penalties. Thus a forecast that generates a positive bias (i.e. overestimation) leads to less curtailments and results in selling more energy. The application of dissuasive penalties would maybe lead to a totally different result. The same type of relationship between the MBE and the economic value of forecasts has already been observed by Ramahatana and David (2019) for the minimization of the costs of a microgrid. Furthermore, very low biases, ranging between -3% and +2%, are observed in this study. This relationship would have not been observed for higher biases because the possible benefits of a strong overestimation will be compensated by its costs. Indeed, an important overestimation of the forecasts results in the impossibility to time-shift the energy because the ESS will always be empty. However, for our case study, if the MBE seems suitable to rank the improvement in terms of gain inside a family, it is not able to give relevant information to compare forecasts originated by different types of model. In Fig. 8(b), a linear relationship between the MAE and the gain seems to appear for the forecasts derived from the ECMWF and NCEP. For these two families of forecasts, an improvement of 1 percentage point in MAE results approximately in an increase of 2 percentage points in gain. Though, the forecasts based on the persistence are not aligned with this relationship. Even if they have clearly worst values of MAE (i.e. at least 5 percentage points more), they do not result in strongly lower gains than the NWP based forecasts. The economic gain defined in this work is proportional to the expected revenue for the user. As a consequence, the linear relationship observed between the MAE and the gain is also valid for the revenue, which is the key indicator for the users. Finally, Fig. 8(c), which plots the gain versus the RMSE, shows that the predominant error metric used in the academic literature to assess the quality of a forecast is unable to provide any relevant information about the added value of forecasts in the considered case study. The results observed in Fig. 8 are in tune with industry requirements. Indeed, users of solar forecasts commonly ask for provision of the MAE. The predominance in the academic literature of the RMSE (Blaga et al., 2019) and by consequence of the the forecast skill based on the RMSE to compare and to rank solar forecasts should be questioned. Given the results of this case study, we assume that a better value is likely reached when all the quality metrics of a forecast (i.e. MBE, MAE and RMSE) are improved simultaneously.

In order to go further, Fig. 9 gives the gain as a function of the two intermediate metrics proposed in this work. The wMAE shows a similar behavior as the MAE. Except for the persistence based forecasts, the gain is almost proportional to the wMAE. With a lower slope and a best alignment of the points, the wMAE is even better to discriminate two forecasts that present close values of wMAE. This result agrees with the approach proposed by Richardson (Richardson, 2000) that defines a cost-loss function based on the cost associated to the consequences of a forecast error. Indeed, the linearity observed between the gain and the MAE and also with the wMAE highlights the underlying structure of the

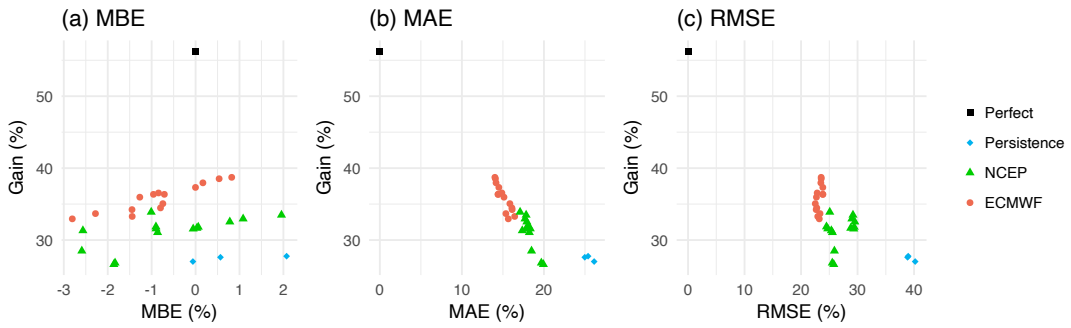

Figure 8: Relationship between economical gain of the ESS managed with day-ahead PV forecasts and error metrics defined into the classical evaluation framework used to assess the quality of the forecasts.

costs associated to an error of forecast. In this specific case study, the cost of a forecast error is almost proportional to the level of this error. And more exactly, weighting the error of forecasts with the spot price offers an interesting approximation of the cost caused by these errors. Finally, the FPF metric, that rewards forecasts with a low level of serial correlation of their errors, does not show any clear relationships with the economical gain. This measure of the forecasting error, initially designed to minimize the LCOE of a firm power generation, seems to not be suitable to study the possibilities offered by the energy arbitrage market.

Looking in detail at the numerical results summarized in Table 4, we can see that forecasts without post-processing give the best economical gains for both ECMWF and NCEP. Indeed, the selected post-treatment methods minimize the RMSE (PAR and NN) or the MBE (WB). But in return, they deteriorate the MAE. For the specific case study of this work, a good post-processing should have reduced the MAE. A last point is also worth noting. The post-processing of the PV forecasts leads in almost all the cases to slightly better results for both quality metrics (i.e. MBE, RMSE and MAE) and value (i.e. economic gain) than the post-processing of the raw GHI provided by the two considered NWPs.

Regarding the influence of the decomposition model, one can easily note that the BRL model has better results than the Erbs model for all the metrics used to assess the quality of the forecasts. Consequently, the use of the BRL model also leads to better a economical gain. The accuracy of the decomposition model is an important factor to take into account. However, for the case study of this work, compared to the choice of the NWP and of the post-processing method, the influence of the decomposition model is of lower-ranking.

7. Conclusion

This work proposes to highlight relationships between metrics used to assess the quality of deterministic forecasts and the added value of these forecasts for the users. A specific case study based on an imaginary PV farm coupled with an ESS aiming to maximise the revenues using the energy arbitrage opportunities has been used. The deterministic solar forecast feeds an optimisation model that generates the charge/discharge profile of the ESS one day-ahead. Even if this case study is inspired by real systems, all the results are obtained by simulating an imaginary system.

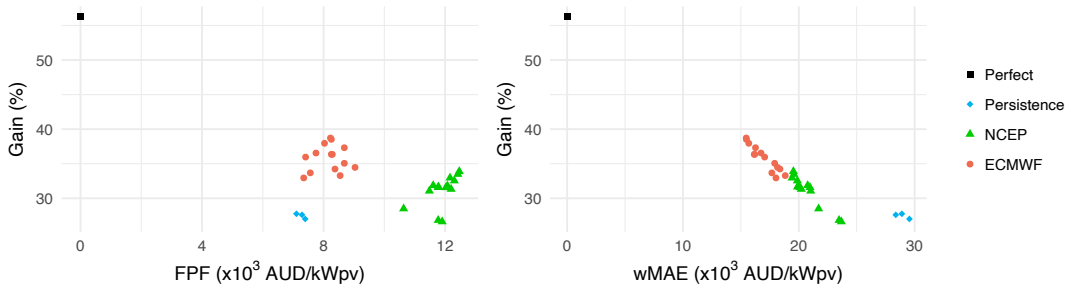

Figure 9: Relationship between economical gain of the ESS managed with day-ahead PV forecasts and the intermediate metrics.

The evaluation framework currently in use by most of the academic researchers of the domain has been used to assess the quality of the forecasts. Here, we used the main ones (i.e. MBE, MAE, RMSE and the forecast skill based on the RMSE) to evaluate quality of our solar forecasts. In addition, we propose to study two intermediate metrics, the weighted MAE (wMAE) and the Firm Power Forecasts (FPF), which are easy to compute, which require few assumptions about the system and which do not need simulation of the system. These intermediate metrics are initially designed to evaluate the value of forecasts under specific conditions.

The results of this work highlight that the metrics based on the Mean Absolute Error (MAE and wMAE) exhibit an almost linear relationship with the economical gain of the forecasts provided by the two tested NWP models. It is shown that an improvement in quality measured by the MAE and wMAE metrics results in an increase of the economical gain. Conversely, the persistence based forecasts do not show the same tendency and lead to poor gain. Furthermore, for the specific case studied in this work, the metrics based on the Root Mean Square Error (RMSE), such as the forecast skill widely used by the academic community, are less efficient to assess the gain provided by an improvement of the forecast quality. This results stress that is it important to consider more than one metric to relevantly assess the quality of a forecast.

In order to validate and to expand the study of the relationships between the metrics designed to assess the quality of solar forecasts and the associated gain for the user, this kind of study should be done on cases based on real systems and also on other types of systems and usages of the forecasts. For instance, ancillary services markets are an important additional source of revenue for solar plants equipped with ESS.

8. Acknowledgments

The authors acknowledge the financial support given by Region Reunion and European Regional Development Fund (FEDER) under the POE-FEDER 2014-2020 (n°2018-1803-0017548) grant.

9. Appendices

Appendix A PAR Post-processing

In the development of MOS equations based on RPR (rolling periodic regression), past measurements (GHI or PV power) and archived NWP model forecast (NCEP or ECMWF) are used with a multivariate regression model to determine the best output minimizing the sum of squared residuals. The regression coefficients (Φ_h) are estimated by the most common estimator using both experimental and observed data. A classical formalism using the Moore–Penrose pseudo-inverse matrix (Penrose, 1956) is used and generates Φ_h for particular predictand according to the time horizon (h). This estimator is theoretically unbiased and consistent if the errors have finite variance and are uncorrelated with the regressors. Considering the time step (30min) and the 72h max forecast horizon, the RPR model is equivalent to 144 AR models (equivalent to the periodic autoregressive model PAR in (Franses and Paap, 1994; Voyant et al., 2018): one model for each h. In the case of GHI predictions (the approach is equivalent for the PV power) and considering the (1×4)-dimensional vector of explanatory variables X ($\mathrm{GHI}_{\mathrm{NWP}}$ for the NWP output concerning the GHI, $\mathrm{GHI}_{\mathrm{CS}}$ for the clear sky model, θ_z for the solar zenith angle and $\widehat{N}$ for the nebulosity predicted by the NWP):

$$X = [\widehat{\mathrm{GHI}}_{\mathrm{NWP}}(t+h), \mathrm{GHI}_{\mathrm{CS}}(t+h), sin(\theta_z(t+h), \widehat{N}(t+h)]. \tag{A.1}$$

And the (1×5)-dimensional column vector Φ_h:

$$\Phi_h = [\phi_{1h}, \phi_{2h}, \phi_{3h}\phi_{4h}, \phi_{5h}]^T. \tag{A.2}$$

The RPR model is equivalent to:

$$\widehat{\mathrm{GHI}}(t+h) = X \times \Phi_h. \text{ for } h = 1:144. \tag{A.3}$$

Rather than operate the training step 1 time for the 144 parameters, a rolling analysis of a time series model is often used to assess the model's stability over time. When analyzing meteorological time series data using a statistical model, a key assumption (which is not really proved) is that the parameters of the model are constant over time. In this study, we propose a parameter estimate over a rolling or moving window of a fixed size through the sample (1 year and operated each day) (Numan, 2016; Yuan and Vanrolleghem, 1999). If the parameters change at some point during the sample, then the rolling estimates should capture this instability and improve the predicor performance. Note that this methodology is possibe due to the low resources required for the use of linear model, more than 50,000 parameters estimated (365×144) in less than 5 seconds with a basic laptop.

To post-process the PV production, slight changes are operate in the inputs. Instead of the GHI, we used the PV production forecasts derived from the NWPs. In the same way, instead of the $\mathrm{GHI}_{\mathrm{CS}}$, we used a PV production under clear sky condition derived from the clear sky irradiances (global, diffuse and direct) provided by the McClear model (Lefèvre et al., 2013) and available for free on the SoDa website (Atmosphere Monitoring Service,

2020). As for the forecasts, the transposition models of Hay and Davies (1980) with an albedo of 0.2 has been used to compute the tilted irradiance.

Appendix B NN Post-processing

Artificial Neural Networks (ANNs or simply NNs) are data driven approaches capable of performing a non-linear mapping between sets of input and output variables. The most popular form of neural network is the so-called multilayer perceptron (MLP) structure (see (Bishop, 1995) for details). The MLP structure consists of an input layer, one or several hidden layers and an output layer. The input layer gathers the model's input vector $\mathbf{x}$ while the output layer yields the model's output y. Fig. 10 represents a one hidden layer MLP.

The hidden layer is characterized by several non-linear functions (or hidden neurons). The non-linear function (also called activation function) is usually the tangent hyperbolic function $f(x) = \frac{e^x - e^{-x}}{e^x + e^{-x}}$. Therefore, a neural network with d inputs, h hidden neurons and a single linear output unit defines a non-linear parameterized mapping from an input vector $\mathbf{x}$ to an output y given by the following relationship:

$$y = y(\mathbf{x}, \mathbf{w}) = \sum_{j=0}^{h} \left(w_j f \left(\sum_{i=0}^{d} w_{ji} x_i \right) \right). \tag{B.1}$$

The NN parameters, denoted by the parameter vector $\mathbf{w} = \{w_j, w_{ji}\}$, govern the non-linear mapping.

The NN parameters $\mathbf{w}$ are estimated during a phase called the training or learning phase. During this phase, the NN is trained using a dataset (called training set) of N input and output examples. The second phase, called the generalization phase, consists of evaluating the ability of the NN to generalize, that is to say, to give correct outputs when it is confronted with examples that were not seen during the training phase. Notice that these examples are part of a data set called test set.

As mentioned above, NNs have the appealing capability to recognize patterns in data. Indeed, NNs are able to approximate any continuous function at an arbitrary accuracy, provided the number of hidden neurons is sufficient. However, it is necessary to match the complexity of the NN to the problem being solved. The complexity determines the generalization capability (measured by the test error) of the model since a NN that is too complex will give poor predictions. In the NN community, this problem is called overfitting. Several techniques like pruning or Bayesian regularization (Bishop, 1995) can be employed to control the NN complexity. In this work, we used the Bayesian Technique in order to control the NN complexity and therefore the generalization capability of the model (Bishop, 1995).

In the present work, an NN is designed to derive the bias correction function. More precisely, the NN output (i.e. the modeled bias $BiasC$) is related to the predicted clear sky index and the solar zenith angle SZA. For instance, the MOS-corrected ECWMF forecasts denoted here ECMWF_c are then obtained by subtracting the modeled bias from the original

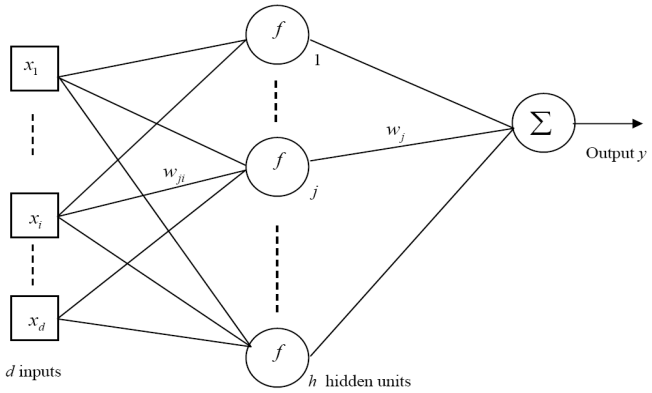

Figure 10: Sketch of a MLP with d inputs and h hidden units, in our case, d=2 (clear sky index and cos(SZA). The output y is the modeled bias correction.

raw ECMWF forecasts ECMWF_o:

$$\text{ECMWF}_c = \text{ECMWF}_o - BiasC. \tag{B.2}$$

Forecasting model	Decomp. model	MBE (%)	RMSE (%)	MAE (%)	FS (%)	wMAE (AUD/kWpv)	FPF (AUD/kWpv)	Economical gain (%) 2016	2020	2025	2030
Perfect	-	0	0	0	100	0	0	55,6	55,8	56,0	56,3
Persistence	-	-0,06	40,2	26,1	-3,3	29,55	7,39	26,5	26,6	26,8	27,0
Persistence_kt	Erbs	0,57	38,8	25	0	28,37	7,29	26,9	27,2	27,4	27,6
Persistence_kt	BRL	2,07	39	25,4	0	28,9	7,11	27,2	27,3	27,5	27,8
NCEP	Erbs	0,78	29,5	17,9	24	19,88	12,3	32,0	32,1	32,3	32,5
NCEP	BRL	1,96	29,2	17,8	25,1	19,57	12,42	33,0	33,1	33,3	33,5
NCEP_BRb	Erbs	0,06	29,4	17,9	24,3	19,97	12,08	31,3	31,4	31,6	31,8
NCEP_BRb	BRL	1,08	29	17,7	25,6	19,42	12,16	32,5	32,6	32,8	33,0
NCEP_Bra	Erbs	-0,05	29,3	18	24,5	20,1	12,03	31,1	31,2	31,4	31,6
NCEP_Bra	BRL	0,03	28,8	17,9	26,1	19,89	11,78	31,2	31,3	31,5	31,7
NCEP_PARb	Erbs	-2,57	25,4	17,4	34,7	20,22	12,2	30,8	30,9	31,1	31,3
NCEP_PARb	BRL	-1,01	25,1	17,1	35,6	19,53	12,47	33,3	33,5	33,7	33,9
NCEP_PARa	Erbs	-0,9	24,7	18,3	36,4	20,97	11,77	31,1	31,2	31,4	31,6
NCEP_PARa	BRL	-0,9	24,5	18,2	37,1	20,77	11,61	31,3	31,5	31,6	31,9
NCEP_NNb	Erbs	-2,59	25,9	18,5	33,3	21,71	10,63	28,0	28,1	28,3	28,5
NCEP_NNb	BRL	-0,86	25,5	18,2	34,4	21,03	11,48	30,6	30,7	30,9	31,1
NCEP_Nna	Erbs	-1,86	25,8	19,9	33,6	23,67	11,9	26,1	26,2	26,4	26,6
NCEP_Nna	BRL	-1,83	25,5	19,7	34,5	23,48	11,77	26,3	26,4	26,6	26,8
ECMWF	Erbs	-0,71	23,9	14,4	38,6	16,19	8,25	35,7	35,9	36,1	36,4
ECMWF	BRL	0,82	23,6	14	39,5	15,46	8,23	38,1	38,2	38,5	38,7
ECMWF_BRb	Erbs	-0,96	23,8	14,4	38,6	16,15	8,29	35,7	35,9	36,1	36,4
ECMWF_BRb	BRL	0,54	23,6	14,1	39,5	15,47	8,26	37,9	38,0	38,3	38,5
ECMWF_Bra	Erbs	0	23,9	14,5	38,6	16,26	8,68	36,7	36,9	37,1	37,3
ECMWF_Bra	BRL	0,17	23,5	14,2	39,7	15,68	8,03	37,3	37,5	37,7	38,0
ECMWF_PARb	Erbs	-2,28	23,4	15,4	39,9	17,67	7,56	33,1	33,3	33,4	33,7
ECMWF_PARb	BRL	-0,84	22,9	14,9	41,3	16,74	7,75	35,9	36,1	36,3	36,5
ECMWF_PARa	Erbs	-0,8	22,8	16,1	41,3	18,16	9,04	33,9	34,0	34,2	34,5
ECMWF_PARa	BRL	-0,74	22,5	15,8	42,2	17,92	8,68	34,5	34,6	34,8	35,1
ECMWF_NNb	Erbs	-2,81	23,2	15,7	40,2	18,03	7,35	32,4	32,5	32,7	32,9
ECMWF_NNb	BRL	-1,27	22,7	15,1	41,7	17,05	7,41	35,3	35,5	35,7	36,0
ECMWF_Nna	Erbs	-1,44	23	16,4	40,9	18,83	8,54	32,7	32,9	33,1	33,3
ECMWF_Nna	BRL	-1,45	22,7	16,1	41,8	18,37	8,38	33,6	33,8	34,0	34,2

Table 4: Forecast quality metrics, intermediate metrics and values of the PV forecasts

References

Abdulla, K., de Hoog, J., Muenzel, V., Suits, F., Steer, K., Wirth, A., Halgamuge, S., 2018. Optimal Operation of Energy Storage Systems Considering Forecasts and Battery Degradation. IEEE Transactions on Smart Grid 9, 2086–2096.

AEMC, 2015. Bidding in Good Faith, Finale Rule Determination.

AEMO Markets, 2018. Guide to generators exemptions and classification of generating units.

AEMO System Capability, 2016. Pre-Dispatch, System Operating Procedure.

Antonanzas, J., Osorio, N., Escobar, R., Urraca, R., Martinez-de Pison, F., Antonanzas-Torres, F., 2016. Review of photovoltaic power forecasting. Solar Energy 136, 78–111.

Antonanzas, J., Perpinan-Lamigueiro, O., Urraca, R., Antonanzas-Torres, F., 2020. Influence of electricity market structures on deterministic solar forecasting verification. Solar Energy , S0038092X20303923.

Atmosphere Monitoring Service, 2020. SoDa (Solar radiation Data),CAMS McClear service for estimating irradiation under clear-sky. `http://www.soda-pro.com/web-services/radiation/cams-mcclear`. Accessed: 2020-03-27.

Aurecon Group, 2020. Hornsdale Power Reserve Year 2 Technical and Market Impact Case Study. Technical Report. Aurecon Group.

Berrada, A., Loudiyi, K., 2016. Operation, sizing, and economic evaluation of storage for solar and wind power plants. Renewable and Sustainable Energy Reviews 59, 1117–1129.
Bertrand, C., Vanderveken, G., Journée, M., 2015. Evaluation of decomposition models of various complexity to estimate the direct solar irradiance over Belgium. Renewable Energy 74, 618–626.
Bishop, C.M., 1995. Neural Networks for Pattern Recognition. Oxford University Press, Inc., USA.
Blaga, R., Sabadus, A., Stefu, N., Dughir, C., Paulescu, M., Badescu, V., 2019. A current perspective on the accuracy of incoming solar energy forecasting. Progress in Energy and Combustion Science 70, 119–144.
Blanc, P., Wald, L., 2010. On the intraday resampling of time-integrated values of solar radiation, in: 10th EMS Annual Meeting (European Meteorological Society), Zurich, Switzerland.
Bridier, L., Hernández-Torres, D., David, M., Lauret, P., 2016. A heuristic approach for optimal sizing of ESS coupled with intermittent renewable sources systems. Renewable Energy 91, 155–165.
Choi, S., Min, S., 2018. Optimal scheduling and operation of the ess for prosumer market environment in grid-connected industrial complex. IEEE Transactions on Industry Applications 54, 1949–1957.
Coimbra, C.F., Kleissl, J., Marquez, R., 2013. Overview of Solar-Forecasting Methods and a Metric for Accuracy Evaluation, in: Solar Energy Forecasting and Resource Assessment. Elsevier, pp. 171–194.
Diagne, M., David, M., Lauret, P., Boland, J., Schmutz, N., 2013. Review of solar irradiance forecasting methods and a proposition for small-scale insular grids. Renewable and Sustainable Energy Reviews 27, 65–76.
Erbs, D., Klein, S., Duffie, J., 1982. Estimation of the diffuse radiation fraction for hourly, daily and monthly-average global radiation. Solar Energy 28, 293–302.
Espinar, B., Wald, L., Blanc, P., Hoyer-Klick, C., Schroedter Homscheidt, M., Wanderer, T., 2011. Project ENDORSE - Excerpt of the report on the harmonization and qualification of meteorological data:Procedures for quality check of meteorological data. Research Report D3.2. Mines ParisTech.
Faraji, J., Abazari, A., Babaei, M., Muyeen, S.M., Benbouzid, M., 2020. Day-ahead optimization of prosumer considering battery depreciation and weather prediction for renewable energy sources. Applied Sciences 10.
Fathima, H., Palanisamy, K., 2015. Optimized Sizing, Selection, and Economic Analysis of Battery Energy Storage for Grid-Connected Wind-PV Hybrid System. Modelling and Simulation in Engineering 2015, 1–16.
Finkel, A., Moses, K., Munro, C., Effeney, T., O'Kane, M., 2017. Independent Review into the Future Security of the National Electricity Market - Blueprint for the Future. Technical Report. Department of the Environment and Energy. Type: dataset.
Franses, P.H., Paap, R., 1994. Model selection in periodic autoregressions†. Oxford Bulletin of Economics and Statistics 56, 421–439. https://onlinelibrary.wiley.com/doi/pdf/10.1111/j.1468-0084.1994.tb00018.x.
Grant Thornton and Clean Energy Pipeline, 2019. Renewable energy discount rate survey results - 2018. Technical Report. Grant Thornton.
Gueymard, C.A., 2009. Direct and indirect uncertainties in the prediction of tilted irradiance for solar engineering applications. Solar Energy 83, 432–444.
Hay, J.E., Davies, J., 1980. Calculations of the solar radiation incident on an inclined surface, in: roceedings of First Canadian Solar Radiation Data Workshop, Canada. pp. 59–72.
Hofmann, M., Seckmeyer, G., 2017. Influence of Various Irradiance Models and Their Combination on Simulation Results of Photovoltaic Systems. Energies 10, 1495.
Holmgren, W.F., Hansen, C.W., Mikofski, M.A., 2018. pvlib python: a python package for modeling solar energy systems. Journal of Open Source Software 3, 884.
Iliadis, Petros, Domalis, Stefanos, Nesiadis, Athanasios, Atsonios, Konstantinos, Chapaloglou, Spyridon, Nikolopoulos, Nikos, Grammelis, Panagiotis, 2019. Advanced energy management system based on pv and load forecasting for load smoothing and optimized peak shaving of islanded power systems. E3S Web Conf. 113, 03001.
IRENA, 2017. Electricity storage and renewables: Costs and markets to 2030. International Renewable Energy Agency, Abu Dhabi, UE.

IRENA, 2019. Renewable Power Generation Costs in 2018. International Renewable Energy Agency, Abu Dhabi, UE.

IRENA, 2020. Electricity Storage Valuation Framework: Assessing system value and ensuring project viability. IRENA, Abu Dhabi, UE. international renewable energy agency edition.

King, D.L., Gonzalez, S., Galbraith, G.M., Boyson, W.E., 2007. Performance Model for Grid-Connected Photovoltaic Inverters. Technical Report SAND2007-5036. Sandia National Laboratories.

Kraas, B., Schroedter-Homscheidt, M., Pulvermüller, B., Madlener, R., 2011. Economic Assessment of a Concentrating Solar Power Forecasting System for Participation in the Spanish Electricity Market. SSRN Electronic Journal .

Lauret, P., Diagne, M., David, M., 2014. A Neural Network Post-processing Approach to Improving NWP Solar Radiation Forecasts. Energy Procedia 57, 1044–1052.

Lauret, P., Lorenz, E., David, M., 2016. Solar Forecasting in a Challenging Insular Context. Atmosphere 7, 18.

Lefèvre, M., Oumbe, A., Blanc, P., Espinar, B., Gschwind, B., Qu, Z., Wald, L., Schroedter-Homscheidt, M., Hoyer-Klick, C., Arola, A., Benedetti, A., Kaiser, J.W., Morcrette, J.J., 2013. McClear: a new model estimating downwelling solar radiation at ground level in clear-sky conditions. Atmospheric Measurement Techniques 6, 2403–2418.

Leutbecher, M., Palmer, T.N., 2008. Ensemble forecasting. Journal of Computational Physics 227, 3515–3539.

Luque, A., Hegedus, S. (Eds.), 2011. Handbook of photovoltaic science and engineering. Wiley, Chichester, West Sussex, U.K. 2nd ed edition. OCLC: ocn656847927.

Luu, N.A., Tran, Q.T., Bacha, S., 2015. Optimal energy management for an island microgrid by using dynamic programming method, in: 2015 IEEE Eindhoven PowerTech, IEEE, Eindhoven, Netherlands. pp. 1–6.

Mayer, M.J., Gróf, G., 2021. Extensive comparison of physical models for photovoltaic power forecasting. Applied Energy 283, 116239.

MINES ParisTech, T., 2020. SoDa (Solar radiation Data), MERRA-2 REANALYSIS. `http://www.soda-pro.com/web-services/meteo-data/merra`. Accessed: 2020-03-27.

Morais, H., Kádár, P., Faria, P., Vale, Z.A., Khodr, H., 2010. Optimal scheduling of a renewable micro-grid in an isolated load area using mixed-integer linear programming. Renewable Energy 35, 151–156.

Mueen, A., Zhu, Y., Yeh, M., Kamgar, K., Viswanathan, K., Gupta, C., Keogh, E., 2017. The fastest similarity search algorithm for time series subsequences under euclidean distance. `http://www.cs.unm.edu/~mueen/FastestSimilaritySearch.html`.

NCEP, 2015. NCEP GFS 0.25 Degree Global Forecast Grids Historical Archive.

Nguyen, M.Y., Yoon, Y.T., Choi, N.H., 2009. Dynamic programming formulation of Micro-Grid operation with heat and electricity constraints, in: 2009 Transmission & Distribution Conference & Exposition: Asia and Pacific, IEEE, Seoul, South Korea. pp. 1–4.

Numan, C., 2016. Intelligent Techniques for Data Analysis in Diverse Settings. IGI Global. Google-Books-ID: mKEoDAAAQBAJ.

Pawel, I., 2014. The Cost of Storage – How to Calculate the Levelized Cost of Stored Energy (LCOE) and Applications to Renewable Energy Generation. Energy Procedia 46, 68–77.

Penrose, R., 1956. On best approximate solutions of linear matrix equations. Mathematical Proceedings of the Cambridge Philosophical Society 52, 17–19.

Perez, M., Perez, R., Rábago, K.R., Putnam, M., 2019. Overbuilding & curtailment: The cost-effective enablers of firm PV generation. Solar Energy 180, 412–422.

Perez, R., Lorenz, E., Pelland, S., Beauharnois, M., Van Knowe, G., Hemker, K., Heinemann, D., Remund, J., Müller, S.C., Traunmüller, W., Steinmauer, G., Pozo, D., Ruiz-Arias, J.A., Lara-Fanego, V., Ramirez-Santigosa, L., Gaston-Romero, M., Pomares, L.M., 2013. Comparison of numerical weather prediction solar irradiance forecasts in the US, Canada and Europe. Solar Energy 94, 305–326.

Pousinho, H., Silva, H., Mendes, V., Collares-Pereira, M., Pereira Cabrita, C., 2014. Self-scheduling for energy and spinning reserve of wind/csp plants by a milp approach. Energy 78, 524–534.

Ramahatana, F., David, M., 2019. Economic optimization of micro-grid operations by dynamic programming with real energy forecast. Journal of Physics: Conference Series 1343, 012067.

Richardson, D.S., 2000. Skill and relative economic value of the ECMWF ensemble prediction system. Quarterly Journal of the Royal Meteorological Society 126, 649–667.

Ridley, B., Boland, J., Lauret, P., 2010. Modelling of diffuse solar fraction with multiple predictors. Renewable Energy 35, 478–483.

Riffonneau, Y., Bacha, S., Barruel, F., Ploix, S., 2011. Optimal Power Flow Management for Grid Connected PV Systems With Batteries. IEEE Transactions on Sustainable Energy 2, 309–320.

Sengupta, M., Habte, A., Gueymard, C., Wilbert, S., Renne, D., 2017. Best Practices Handbook for the Collection and Use of Solar Resource Data for Solar Energy Applications: Second Edition. Technical Report NREL/TP-5D00-68886, 1411856. NREL.

Short, W., Packey, D.J., Holt, T., 2005. A manual for the economic evaluation of energy efficiency and renewable energy technologies. University Press of the Pacific, Honolulu, Hawaii. repr. from the 1995 ed edition. OCLC: 636197534.

Sobri, S., Koohi-Kamali, S., Rahim, N.A., 2018. Solar photovoltaic generation forecasting methods: A review. Energy Conversion and Management 156, 459–497.

Voyant, C., Gooijer], J.G.D., Notton, G., 2018. Periodic autoregressive forecasting of global solar irradiation without knowledge-based model implementation. Solar Energy 174, 121 – 129.

Wittmann, M., Breitkreuz, H., Schroedter-Homscheidt, M., Eck, M., 2008. Case Studies on the Use of Solar Irradiance Forecast for Optimized Operation Strategies of Solar Thermal Power Plants. IEEE Journal of Selected Topics in Applied Earth Observations and Remote Sensing 1, 18–27.

Wouters, C., Fraga, E.S., James, A.M., 2015. An energy integrated, multi-microgrid, MILP (mixed-integer linear programming) approach for residential distributed energy system planning – A South Australian case-study. Energy 85, 30–44.

Yang, D., 2019. Standard of reference in operational day-ahead deterministic solar forecasting. Journal of Renewable and Sustainable Energy 11, 053702.

Yang, D., Alessandrini, S., Antonanzas, J., Antonanzas-Torres, F., Badescu, V., Beyer, H.G., Blaga, R., Boland, J., Bright, J.M., Coimbra, C.F., David, M., Frimane, , Gueymard, C.A., Hong, T., Kay, M.J., Killinger, S., Kleissl, J., Lauret, P., Lorenz, E., van der Meer, D., Paulescu, M., Perez, R., Perpiñán-Lamigueiro, O., Peters, I.M., Reikard, G., Renné, D., Saint-Drenan, Y.M., Shuai, Y., Urraca, R., Verbois, H., Vignola, F., Voyant, C., Zhang, J., 2020. Verification of deterministic solar forecasts. Solar Energy , S0038092X20303947.

Yang, D., Wu, E., Kleissl, J., 2019a. Operational solar forecasting for the real-time market. International Journal of Forecasting 35, 1499–1519.

Yang, Y., Bremner, S., Menictas, C., Kay, M., 2019b. A mixed receding horizon control strategy for battery energy storage system scheduling in a hybrid pv and wind power plant with different forecast techniques. Energies 12.

Yuan, J.Q., Vanrolleghem, P.A., 1999. Rolling learning-prediction of product formation in bioprocesses. Journal of Biotechnology 69, 47 – 62.

Zhang, X., Lu, N., Jiang, H., Yao, L., 2020. Evaluation of reanalysis surface incident solar radiation data in china. Scientific Reports 10.

Zhao, H., Wu, Q., Hu, S., Xu, H., Rasmussen, C.N., 2015. Review of energy storage system for wind power integration support. Applied Energy 137, 545–553.